ABCResearch

Arch Basic Clin Res 2024; 6(2): 82-89 • DOI: 10.5152/ABCR.2024.23220

Original Article

The Relationship Between Tuber Load and White Matter Pathways in Children with Tuberous Sclerosis Complex: A Diffusion Tensor Imaging Study

Bahar Atasoy

Department of Radiology, Bezmialem Vakıf University Faculty of Medicine, İstanbul, Türkiye

Cite this article as: Atasoy B. The relationship between tuber load and white matter pathways in children with tuberous sclerosis complex: A diffusion tensor imaging study. *Arch Basic Clin Res.* 2024;6(2):82-89.

ORCID ID of the author: B.A. 0000-0002-5393-5876.

ABSTRACT

Objective: The aim of our study was to investigate whether there are diffusion tensor imaging (DTI) changes in the white matter pathways and to determine its relationship with tuber load and corpus callosum volume (CCV).

Methods: Our study included 24 children with tuberous sclerosis complex (TSC) (group 1) and 30 healthy controls (group 2). Total tuber load and CCV were calculated. The fractional anisotropy (FA) and apparent diffusion coefficient (ADC) values of the 15 different white matter tracts were measured. The correlation between the total tuber volume, CCV, and white matter changes was investigated.

Results: The ADC values of forceps major and corticospinal tract (CST) were increased in group 1 compared to group 2. The FA values of corpus callosum splenium (CCS) were decreased in group 1 compared to group 2. There was a positive correlation between ADC values at corona radiata (CR), corpus callosum genu (CCG), forceps minor, forceps major, and tuber volume. There was a negative correlation between FA values at the anterior limb internal capsule (ALIC) and tuber volume. There was a negative correlation between the total tuber volume and CCV. There was a negative correlation between ADC values at CCG, ALIC, middle cerebellar pedicle (MCP), and CCV. There was a positive correlation between FA values at CCG and CCV.

Conclusion: We hypothesized that the white matter microstructure was prominently affected in TSC subjects, this might resulted in decrease in CCV, and it is correlated with the tuber load. Furthermore, more comprehensive studies are needed to determine the relationship between the neurocognitive dysfunction, DTI metrics, and tuber and CCV.

Keywords: Tuberous sclerosis, diffusion tensor imaging, fractional anisotropy, apparent diffusion coefficient, tuber load, corpus callosum volume

INTRODUCTION

A mutation in the TSC1 or TSC2 genes causes tuberous sclerosis complex (TSC), an autosomal genetic condition. Tuberous sclerosis complex is a multisystemic disease manifesting with central nervous system (CNS) lesions referred to as hamartomas.[1] Three forms of CNS lesions have been identified in magnetic resonance imaging (MRI): cortical tubers (90%), subependymal nodules (SENs) (80%), and subependymal giant cell astrocytoma (5%-15%).[2,3] Moreover, autistic behavior, neurocognitive dysfunction, epilepsy, along with emotional issues including anxiety and self-injurious conduct, are among the neurological and psychiatric symptoms that commonly co-occur in patients; these conditions are collectively known as TSC-associated neuropsychiatric disorders.[3]

Diffusion tensor imaging (DTI) can provide details on the integrity of the white matter (WM) microstructure by analyzing the average diffusion of water at the microscopic level of the tissue.[4] Fractional anisotropy (FA) and apparent diffusion coefficient (ADC) are the two most commonly utilized DTI metrics. In the literature, most of the previous DTI studies were mostly focused on cortical tuber and white matter lesions, and there are not many studies evaluating normal-appearing white matter (NAWM)

Corresponding Author: Bahar Atasoy, **E-mail:** bahar_atasoy@hotmail.com

Received: September 27, 2023
Revision Requested: January 13, 2024
Last Revision Received: February 6, 2024
Accepted: April 19, 2024
Publication Date: May 27, 2024

with DTI and investigating the relationship between white matter changes and tuber load.[5,6]

Several studies demonstrated higher ADC and lower FA values in the WM hamartomas compared to contralateral NAWM. These DWI alterations are attributed to the disorganization of the normal cortical architecture, hypomyelination, gliosis, and heterotrophic cells in the WM lesions.[7-9] Moreover, DTI studies pointed out that the white matter changes were mainly observed in the corpus callosum in TSC patients.[5,10,11]

The aim of our study is to investigate the possible DTI alterations in the white matter pathways and to determine their relationship with tuber load and corpus callosum volume.

MATERIAL AND METHODS

Participants

The study was approved by the ethical committee of Bezmialem Foundation University, Türkiye (E-54022451-050.05.04-117247; date: 31.07.2023). Our study included 24 children with TSC (group 1) (13 females, 11 males; mean age 9.83 ± 5.82) and 30 age-matched healthy controls (group 2) (20 females, 10 males; mean age 8.93 ± 4.54). The patients' established diagnosis of TSC is based on clinical and imaging criteria. All of the patients had characteristic TSC lesions, such as SENs, cortical/subcortical tubers, and abnormalities of the white matter. The study's control subjects had normal MR imaging without any history of neurologic disorders. While forming the control group, those who presented with headache complaints and had normal brain MRIs were included in the study. The control group is selected from the patients without any neurological abnormalities following the physical examinations of a registered pediatric neurologist. Those with a history of head trauma, cerebrovascular disease, cranial surgery, and degenerative diseases were excluded from the study. Informed consent was obtained from all patients and their parents.

MAIN POINTS

- In TSC, tuber-like pathology is widely distributed in the white matter, and their detection is important for determining the course of the disease.
- Our DTI findings may suggest that microstructural damage to the white matter (WM) in patients with TSC is mostly prominent in the commissural and projection fibers, and may be related to the demyelination, axonal degeneration, and gliosis.
- Corpus callosum (CC) volume was found to be significantly lower in patients with TSC, and this decrease shows a positive correlation with tuber load. We hypothesized that DTI abnormalities in the WM pathways may lead to a decrease in CC volume.
- As a conclusion, we hypothesized that the white matter microstructure was prominently affected in TSC subjects, this might result in decrease in CC volume, and it is correlated with the tuber load.

MR Imaging

A 1.5T MRI system (Siemens Avanto, Germany) with a maximum gradient power of 43 mT/m was performed for the examination of the subjects.

The MRI protocol in our study consisted of axial T1 (TR: 500/TE: 87 ms), fluid-attenuated inversion-recovery (FLAIR; TR: 8.000/TE: 118/TI: 23.687 ms), T2 (TR: 4.280/TE: 91 ms), MPRAGE 3D T1 (three-dimensional magnetization-prepared rapid-acquisition gradient-echo with an isotropic voxel resolution of 1 mm), sagittal T2, and coronal FLAIR images.

The DTI protocol included SE-EPI images, TR/TE = 6.000/89 ms, 30 gradient directions, b = 0 s/mm^2 and b = 1000s/mm^2, matrix: 128 × 128, 5 mm slice thickness, and FOV of 230 mm. Diffusion tensor imaging analysis was performed using an area region of interest (ROI)-based technique. Values were calculated from the reconstructed ADC and color-coded FA maps in the workstation (software version 2.0; Siemens). An experienced radiologist placed all ROIs concurrently on an axial color-encoded FA map (B.A.). Region of interests were placed on the 15 different white matter tracts: cingulum (CG), corona radiata (CR), genu–splenium of the corpus callosum (GCC–SCC), superior longitudinal fasciculus–inferior longitudinal fasciculus (SLF–ILF), superior fronto-occipital fasciculus (SFOF), anterior limb of the internal capsule–posterior limb of the internal capsule (ALIC–PLIC), forceps minor–major, external capsule, middle cerebellar pedicles (MCP), corticospinal tracts (CST), and central tegmental tracts (CTT). The FA and ADC values of the groups were compared (Figures 1-3). T2 and FLAIR images are interpreted by a neuroradiologist (B.A.) for detecting the tubers.

All segmentations and the volumetric analysis of the corpus callosum and tuber lesions have been done on the 3D Slicer software (version 5.2.2) manually.[12] The number of cortical and subcortical tubers was determined. The margins of the tubers are marked and their volumes are calculated on the axial FLAIR images (Figures 1-3), while the corpus callosum margin is outlined, and its volume is calculated on the sagittal T2W images (Figures 1-3). Volumetric lesion analysis was

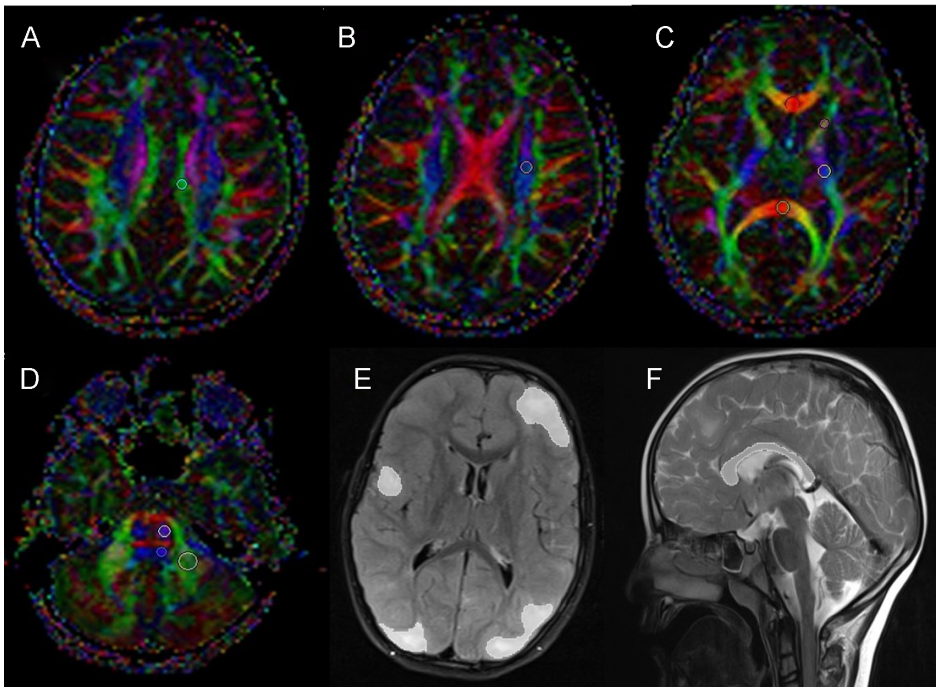

Figure 1. Axial color-coded FA maps show the placement of the ROIs (region of interest) on the left cingulum (A), corona radiata (B), genu and splenium of corpus callosum, anterior and posterior limb of internal capsule (C), and corticospinal tracts, central tegmental tracts, and middle cerebellar pedicle (D). Axial FLAIR images show cortical/subcortical tubers in the bilateral cerebral hemispheres, which have been outlined manually to calculate the volume of the cortical/subcortical tubers (E). The corpus callosum volume was outlined and calculated on the sagittal T2W images (F).

analyzed in cubic centimeters (cm^3). The brain's total tuber load was determined. The correlation between the tuber volume, corpus callosum volume, and white matter changes was investigated.

Statistical Analysis

The Shapiro–Wilk's test was used for the variables' distribution evaluation. Descriptive statistics were presented as mean ± standard deviation and median (minimum–maximum). Independent samples *t*-test, Spearman correlation coefficient, and Mann–Whitney *U*-test were used. The level of significance was taken as α = 0.05. Analyses were done by International Business Machiness (IBM) Statistical Package for the Social Sciences (SPSS), Version 28.0 (IBM SPSS Corp.; Armonk, NY, USA).

RESULTS

The FA and ADC values acquired from different WM tracts in the patients with TSC (group 1) and controls (group 2) are presented in Table 1.

There was a significant difference between group 1 and group 2 in terms of ADC values at the forceps major and CST (*P* = .045, *P* = .018 respectively). The ADC values of forceps major and CST were increased in group 1. In addition, the FA values of CCS were decreased in group 1 in comparison to group 2 (*P* = .026).

The calculated mean total tuber volume was 9803 cm^3 (min–max; 0, 477–81500). The median total tuber number was 12, 50 (min–max; 1–33).

There was a positive correlation between ADC values at CR, CCG, forceps minor, forceps major, and tuber volume (*P* = .014; *r* = 0.494, *P* = .014; *r* = 0.497, *P* = .001; *r* = 0.613, *P* = .024; *r* = 0.458, respectively). In addition, there was a negative correlation between FA values at ALIC and tuber volume (*P* = .035; *r* = −0.433) (Table 2).

There was a positive correlation between ADC values at CR, CCG, forceps major, forceps minor, and tuber number (*P* = .024; *r* = 0.459, *P* = .007; *r* = 0.535, *P* = .020; *r* = 471, *P* = .020; *r* = 471, respectively). Also, there was a negative correlation between FA values at ALIC and tuber number (*P* = .028; *r* = −0.448).

The mean CC volume of group 1 was 2939 ± 627 cm^3, and group 2 was 3484 ± 503 cm^3. Group 1 had significantly decreased CC volume in comparison to group 2 (*P* = .001). There was a negative correlation between the tuber volume and CC volume (*P* = .006, *r* = −0.548).

There was a negative correlation between ADC values at CCG, ALIC, MCP, and CC volume (*P* = .033, *r* = −0.436, *P* = .021, *r* = −0.470, *P* = .044, *r* = −0.415, respectively). In addition, a positive correlation was found between

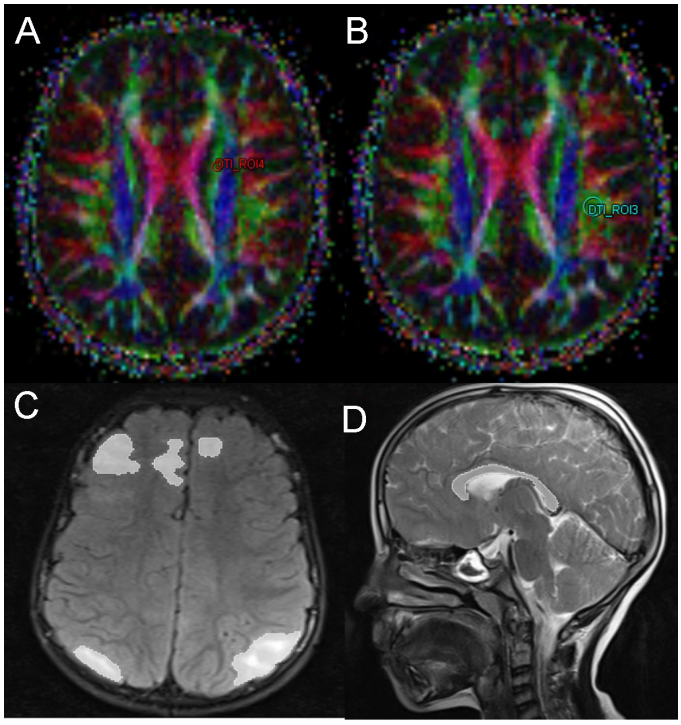

Figure 2. Axial color-coded FA maps show the placement of the ROIs (region of interest) on the left superior frontooccipital fasciculus (SFOF) (A) and superior longitudinal fasciculus (SLF) (B). Axial FLAIR images show cortical/subcortical tubers in the bilateral cerebral hemispheres, which have been outlined manually to calculate the volume of the cortical/subcortical tubers (C). The corpus callosum volume was outlined and calculated on the sagittal T2W images (D).

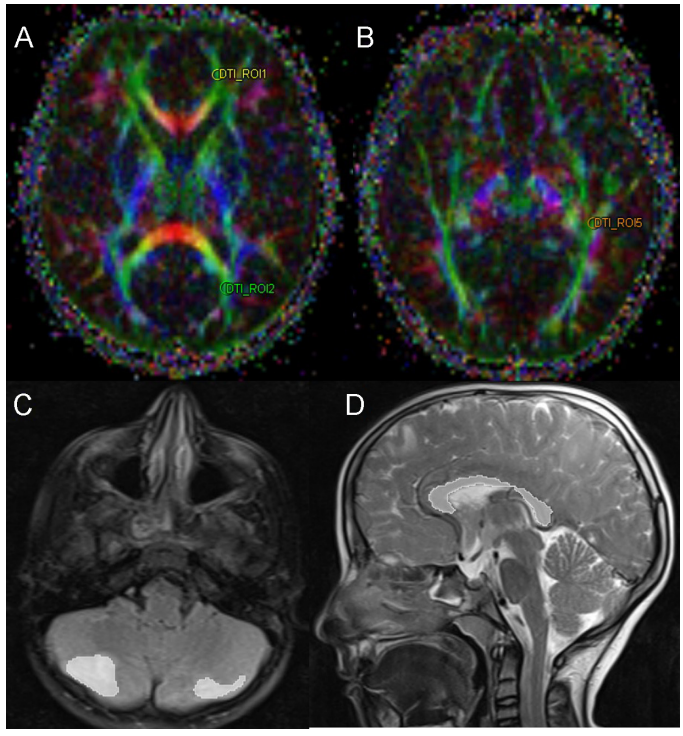

Figure 3. Axial color-coded FA maps show the placement of the ROIs (region of interest) on the left forceps major–minor (A) and inferior longitudinal fasciculus (ILF) (B). Axial FLAIR images show cortical/subcortical tubers in the bilateral cerebellar hemispheres, which have been outlined manually to calculate the volume of the cortical/subcortical tubers (C). The corpus callosum volume was outlined and calculated on the sagittal T2W images (D).

FA values at CCG and CC volume (P = .009, r = 0.524) (Table 3).

DISCUSSION

The TSC hamartomas' histological analysis has revealed characteristics of aberrant neuronal and astrocyte overgrowth and cell enlargement.[13-17] It is well recognized that widespread tuber-like pathology exists in the white matter below the level of detection of conventional MRI.[18] Since the DTI changes in white matter tracts may be associated with neurocognitive dysfunctions, their detection is important in terms of determining the course of the disease.[10,11]

In the literature, several studies demonstrated DTI alterations of the tuber lesions, perilesional areas, and contralateral white matter.[7-9,19] Dogan et al.[19] pointed out decreased FA values and increased ADC, AD, and RD values in tubers compared to those obtained from the contralateral normal regions. They explained these findings by the proliferation of hamartomas, as well as by the depletion and disorganization of myelin sheaths. Moreover, Karadag et al.[7] have shown higher ADC values within tubers compared to a normal control group, together with increased ADC and decreased FA values in WM abnormalities and perilesional WM compared to the contralateral side and normal controls. The removal of structural barriers to water motion in the WM lesions and perilesional regions was assumed to be a result of hypomyelination, gliosis, and heterotopic cells, which would result in DTI alterations.

In our study, we found increased ADC values in the forceps major and CST. Moreover, we found decreased FA values in the CCS in TSC patients. The corpus callosum in the brain's major commissural tract connects the left and right hemispheres of the brain. Additionally, the CST has projection tracts that link the brainstem, thalamus, and spinal cord to the cerebrum. Moreover, a white matter fiber bundle known as the posterior forceps, sometimes known as the forceps major, connects the occipital lobes with the corpus callosum's splenium. Makki et al.[20] demonstrated increased ADC and decreased FA values in the corpus callosum, external and internal capsules. They explained these changes by gliosis and myelination abnormalities, which may be

Table 1. Comparison of ADC and FA Values Between Patients with TSC (Group 1) and Controls (Group 2)

	ADC ($\times 10^{-3}$ mm^2/s)			FA		
Locations	**Group 1 (n = 24)**	**Group 2 (n = 30)**	***P***	**Group 1 (n = 24)**	**Group 2 (n = 30)**	***P***
Cingulum	0.836 ± 0.104	0.811 ± 0.055	.305	0.535 ± 0.128	0.550 ± 0.089	.621
Corona radiata	0.799 ± 0 065	0.770 ± 0.051	.081	0.591 ± 0.090	0.523 ± 0.071	**.003***
SLF	0.789 ± 0.078	0.786 ± 0.058	.868	0.530 ± 0.100	0.517 ± 0.051	.562
ILF	0.895 ± 0.069	0.858 ± 0.080	.085	0.484 ± 0.086	0.463 ± 0.098	.429
SFOF	0.847 ± 0.108	0.811 ± 0.089	.193	0.503 ± 0.112	0.432 ± 0.077	**.013***
CCG	0.893 ± 0.108	0.885 ± 0.062	.725	0.761 ± 0.088	0.780 ± 0.051	.330
CCS	0.870 ± 0.096	0.844 ± 0.076	.271	0.778 ± 0.071	0.817 ± 0.043	**.026***
ALIC	0.800 ± 0.079	0.781 ± 0.058	.304	0.524 ± 0.075	0.530 ± 0.080	.756
PLIC	0.758 ± 0.065	0.780 ± 0.059	.187	0.679 ± 0.042	0.736 ± 0.051	**<.001***
External capsule	0 817 ± 0.074	0.799 ± 0.053	.317	0.386 ± 0.078	0.401 ± 0.077	.489
Forceps minor	0.862 ± 0.087	0.834 ± 0.052	**.045***	0.541 ± 0.076	0.518 ± 0.094	.203
Forceps major	0.902 ± 0.125	0.846 ± 0.073	.166	0.699 ± 0.106	0.660 ± 0.112	.335
CST	0.821 ± 0.105	0.764 ± 0.045	**.018***	0.529 ± 0.115	0.520 ± 0.062	.742
CTT	0.853 ± 0.109	0.832 ± 0.069	.429	0.588 ± 0.121	0.600 ±0.099	.713
MCP	0.747 ± 0.062	0.749 ± 0.046	.905	0.718 ± 0.082	0.729 ± 0.048	.572

Data are presented as mean ± standard deviation.
ADC, apparent diffusion coefficient; ALIC, anterior limbs of internal capsule; CST, corticospinal tracts; FA, fractional anisotropy; GCC, genu of corpus callosum; ILF, inferior longitudinal fasciculus MCP, middle cerebellar pedicle; *n*, number of subjects; PLIC, posterior limbs of internal capsule; SLF, superior longitudinal fasciculus; SFOF, superior frontooccipital fasciculus; SCC, splenium of corpus callosum; TPF, transverse pontine fibers.
*Shows statistically significant results.

Table 2. Correlation Between Total Tuber Volume and DTI Indices of Different White Matter Tracts

Locations	**Correlation**	**ADC**	**FA**
Cingulum	Tuber volume	$r = 0.196$ ($P = .359$)	$r = -0.302$ ($P = .152$)
Corona radiata	Tuber volume	$r = 0.494$ **($P = .014$)***	$r = 0.175$ ($P = .414$)
SLF	Tuber volume	$r = 0.161$ ($P = .452$)	$r = -0.145$ ($P = .498$)
ILF	Tuber volume	$r = -0.071$ ($P = .741$)	$r = -0.119$ ($P = .579$)
SFOF	Tuber volume	$r = 0.234$ ($P = 0.271$)	$r = 0.028$ ($P = .897$)
CCG	Tuber volume	$r = 0.497$ **($P = .014$)***	$r = -0.272$ ($P = .199$)
CCS	Tuber volume	$r = 0.197$ ($P = .357$)	$r = -0.303$ ($P = .151$)
ALIC	Tuber volume	$r = 0.332$ ($P = .113$)	$r = -0.433$ **($P = .035$)***
PLIC	Tuber volume	$r = 0.105$ ($P = .625$)	$r = 0.190$ ($P = .374$)
External capsule	Tuber volume	$r = 0.204$ ($P = .340$)	$r = -0.231$ ($P = .278$)
Forceps minor	Tuber volume	$r = 0.613$ **($P = .001$)***	$r = -0.164$ ($P = .445$)
Forceps major	Tuber volume	$r = 0.458$ **($P = .024$)***	$r = -0.287$ ($P = .173$)
CST	Tuber volume	$r = 0.077$ ($P = .722$)	$r = -0.035$ ($P = .872$)
CTT	Tuber volume	$r = 0.263$ ($P = .214$)	$r = -0.109$ ($P = .613$)
MCP	Tuber volume	$r = 0.306$ ($P = .148$)	$r = -0.274$ ($P = .196$)

ADC, apparent diffusion coefficient; ALIC, anterior limbs of internal capsule; CST, corticospinal tracts; FA, fractional anisotropy; GCC, genu of corpus callosum; ILF, inferior longitudinal fasciculus; MCP, middle cerebellar pedicle; PLIC, posterior limbs of internal capsule; SLF, superior longitudinal fasciculus; SFOF, superior frontooccipital fasciculus; SCC, splenium of corpus callosum; TPF, transverse pontine fibers.
*Shows statistically significant results.

Table 3. Correlation Between Corpus Callosum Volume and DTI Indices of Different White Matter Tracts

Locations	Correlation	ADC	FA
Cingulum	Corpus callosum volume		$r = 0.375$ ($P = .098$)
Corona radiata	Corpus callosum volume	$r = -0.285$ ($P = .177$)	$r = 0.028$ ($P = .897$)
SLF	Corpus callosum volume	$r = -0.349$ ($P = .095$)	$r = -0.039$ ($P = .856$)
ILF	Corpus callosum volume	$r = -0.07$ ($P = .731$)	$r = -0.155$ ($P = .470$)
SFOF	Corpus callosum volume	$r = -0.148$ ($P = .491$)	$r = 0.030$ ($P = .888$)
CCG	Corpus callosum volume	$r = -0.436$ **($P = .033$)***	$r = 0.524$ **($P = .009$)***
CCS	Corpus callosum volume	$r = -0.192$ ($P = .369$)	$r = 0.117$ ($P = 0.585$)
ALIC	Corpus callosum volume	$r = -0.470$ **($P = .021$)***	$r = 0.231$ ($P = .277$)
PLIC	Corpus callosum volume	$r = -0.244$ ($P = .250$)	$r = 0.051$ ($P = .813$)
External capsule	Corpus callosum volume	$r = 0.067$ ($P = .757$)	$r = 0.216$ ($P = .310$)
Forceps minor	Corpus callosum volume	$r = -0.401$ ($P = .052$)	$r = 0.094$ ($P = .662$)
Forceps major	Corpus callosum volume	$r = -0.362$ ($P = .082$)	$r = 0.258$ ($P = .224$)
CST	Corpus callosum volume	$r = 0.010$ ($P = .965$)	$r = 0.155$ ($P = .469$)
CTT	Corpus callosum volume	$r = -0.017$ ($P = .939$)	$r = -0.074$ ($P = .731$)
MCP	Corpus callosum volume	$r = -0.415$ **($P = .044$)***	$r = -0.042$ ($P = .846$)

ADC, apparent diffusion coefficient; ALIC, anterior limbs of internal capsule; CST, corticospinal tracts; FA, fractional anisotropy; GCC, genu of corpus callosum; ILF, inferior longitudinal fasciculus; MCP middle cerebellar pedicle; PLIC, posterior limbs of internal capsule; SLF, superior longitudinal fasciculus; SFOF, superior frontooccipital fasciculus; SCC, splenium of corpus callosum; TPF, transverse pontine fibers.
*Shows statistically significant results.

responsible for axonal microstructural alterations. Zikou et al.[21] reported increased axial diffusivity in children with tuberous sclerosis complex in the superior and anterior corona radiata, the superior longitudinal fascicle, the inferior fronto-occipital fascicle, the uncinate fascicle, and the anterior thalamic radiation in a TBSS study. They attributed these WM alterations to axonal integrity reduction. Increased radial diffusivity in normal-appearing white matter in TSC patients has been shown by Peters et al.[22] to be indicative of either inadequate myelination (thickness, integrity, or permeability) or an increased amount of extracellular material, which compromises the biological barrier to diffusion in the radial direction. Moreover, Baumer et al.[11] reported that the corpus callosum's DTI measurements are cumulatively linked to concomitant neurological symptoms in TSC. In addition, Sato et al.[10] demonstrated reduced FA values in the inferior frontal occipital fasciculus (IFOF), SLF, uncinate fasciculus (UF), ILF, and GCC in the TSC. Fractional anisotropy is used to measure the white matter's coherence quantitatively. Axon structure that is physiologically myelinated and well organized is indicated by higher FA levels. Reduced FA values in CCS in our study may be related to axonal degeneration and demyelination. Moreover, increased ADC values in forceps major and CST may highlight the decrease in axonal quantity and increase in extracellular fluid due to destruction in myelin sheath. Coban et al.[23] pointed out similar results with these DTI findings in normal appearing brain parenchyma by using synthetic MRI and explained these findings by underlying myelin and/or axonal structural alterations in TSC patients.

In this study, we found a positive correlation between the ADC values of CR, CCG, forceps minor, and tuber volume and number. Moreover, we detected a negative correlation between FA values at the ALIC and tuber volume and number. Simao et al.[5] reported a negative correlation between the FA values of CCS and total tuber volume and a positive correlation between trace in the CCG and CCS and total tuber volume. Cesme et al.[6] demonstrated a negative correlation between the FA values of CCS and a positive correlation between the ADC values of CCS and tuber load. In addition, they reported increased ADC and FA values in the GCC, SCC, and internal capsules. Similar to previous studies, our findings suggested that the DTI indices of CC and IC were mostly prominent and correlated with the tuber volume. In addition to previous studies, we pointed out the DTI alterations at the CR and forceps minor. The CR is a projection fiber that continues inferiorly as the internal capsule. Our findings may suggest that the microstructural damage of the WM in patients with TSC is mostly prominent in the commissural and projection fibers and may be related to demyelination, axonal degeneration, and gliosis in these WM microstructures. Moreover, we suggested that tuber

number is a sensitive marker for assessing white matter alterations, as both tuber volume and number exhibit the same DTI metrics in this study.

In our study, CC volume was found to be significantly lower in patients with TSC, and this decrease shows a positive correlation with tuber load. This finding supported the DTI changes observed in the CC in patients with TSC. Moreover, a negative correlation was detected between the ADC values of CCG, ALIC, MCP, and CC volume. Also, a positive correlation was found between FA values at CCG and CC volume. Our findings possibly reflect the presence of disorganized myelin sheaths and gliosis, mainly in these WM microstructures, and this damage correlated with the CC volume. We hypothesized that the DTI abnormalities in the WM pathways may result in a decrease in CC volume since the CC is the principal commissural region of the brain and contains white matter tracts that link the left and right cerebral hemispheres.

There are some drawbacks to our study. The first limitation is that the tuber lesions are not evaluated according to their lobar and hemispheric distribution. The second drawback is that ROI-based methods are used to make DTI measurements. The margin of error in ADC and FA readings will be kept to a minimum by using voxel-based measurement techniques. The third drawback is the lack of research on the connection between DTI measures and neurocognitive functions.

In conclusion, we hypothesized that the white matter microstructure was prominently affected in TSC subjects; this might result in decrease in CC volume, correlated with the tuber load. Further, studies that are more comprehensive are needed to determine the relationship between neurocognitive dysfunction, DTI metrics, and tuber and CC volume.

Ethics Committee Approval: The study was approved by the ethical committee of Bezmialem Foundation University, Türkiye (number: E-54022451-050.05.04-117247; date: 31.07.2023).

Informed Consent: Informed consent was obtained from all patients and their parents.

Peer-review: Externally peer-reviewed.

Declaration of Interests: The author has no conflict of interest to declare.

Funding: The author declared that this study has received no financial support.

REFERENCES

1. Müller AR, Luijten MAJ, Haverman L, et al. Understanding the impact of tuberous sclerosis complex: development and validation of the TSC-PROM. *BMC Med*. 2023;21(1):298. [CrossRef]
2. DiMario FJ Jr. Brain abnormalities in tuberous sclerosis complex. *J Child Neurol*. 2004;19(9):650-657. [CrossRef]
3. Northrup H, Koenig MK, Pearson DA, Au K-S. *Tuberous Sclerosis Complex. NCBI Bookshelf*. Seattle: WA; 2015.
4. Gultekin MA, Cesme DH, Karaman O, et al. Brain diffusion tensor imaging findings in Hashimoto's thyroiditis. *J Neuroimaging*. 2021;31(1):215-221. [CrossRef]
5. Simao G, Raybaud C, Chuang S, Go C, Snead OC, Widjaja E. Diffusion tensor imaging of commissural and projection white matter in tuberous sclerosis complex and correlation with tuber load. *AJNR Am J Neuroradiol*. 2010;31(7):1273-1277. [CrossRef]
6. Cesme DH. Evaluation of the relationship between corpus callosum and internal capsule and tuber load in patients with tuberous sclerosis complex by diffusion tensor imaging. *Ann Med Res*. 2021;28(3):575-578. [CrossRef]
7. Karadag D, Mentzel HJ, Güllmar D, et al. Diffusion tensor imaging in children and adolescents with tuberous sclerosis. *Pediatr Radiol*. 2005;35(10):980-983. [CrossRef]
8. Garaci FG, Floris R, Bozzao A, et al. Increased brain apparent diffusion coefficient in tuberous sclerosis. *Radiology*. 2004;232(2):461-465. [CrossRef]
9. Peng SSF, Lee WT, Wang YH, Huang KM. Cerebral diffusion tensor images in children with tuberous sclerosis: a preliminary report. *Pediatr Radiol*. 2004;34(5):387-392. [CrossRef]
10. Sato A, Tominaga K, Iwatani Y, et al. Abnormal white matter microstructure in the limbic system is associated with tuberous sclerosis complex-associated neuropsychiatric disorders. *Front Neurol*. 2022;13:782479. [CrossRef]
11. Baumer FM, Peters JM, Clancy S, et al. Corpus callosum white matter diffusivity reflects cumulative neurological comorbidity in tuberous sclerosis complex. *Cereb Cortex*. 2018;28(10):3665-3672. [CrossRef]
12. Fedorov A, Beichel R, Kalpathy-Cramer J, et al. 3D Slicer as an image computing platform for the quantitative imaging network. *Magn Reson Imaging*. 2012;30(9):1323-1341. [CrossRef]
13. Hsieh CCJ, Lo YC, Li SJ, et al. Detection of endophenotypes associated with neuropsychiatric deficiencies in a mouse model of tuberous sclerosis complex using diffusion tensor imaging. *Brain Pathol*. 2021;31(1):4-19. [CrossRef]
14. Curatolo P, Moavero R. mTOR inhibitors in tuberous sclerosis complex. *Curr Neuropharmacol*. 2012;10(4):404-415. [CrossRef]
15. Laplante M, Sabatini DM. MTOR signaling in growth control and disease. *Cell*. 2012;149(2):274-293. [CrossRef]
16. Han JM, Sahin M. TSC1/TSC2 signaling in the CNS. *FEBS Lett*. 2011;585(7):973-980. [CrossRef]
17. Grajkowska W, Kotulska K, Jurkiewicz E, Matyja E. Brain lesions in tuberous sclerosis complex. [Review]. *Folia Neuropathol*. 2010;48(3):139-149.
18. Taoka T, Aida N, Fujii Y, et al. White matter microstructural changes in tuberous sclerosis: evaluation by neurite orientation dispersion and density imaging (NODDI) and diffusion tensor images. *Sci Rep*. 2020;10(1):436. [CrossRef]
19. Dogan MS, Gumus K, Koc G, et al. Brain diffusion tensor imaging in children with tuberous sclerosis. *Diagn Interv Imaging*. 2016;97(2):171-176. [CrossRef]
20. Makki MI, Chugani DC, Janisse J, Chugani HT. Characteristics of abnormal diffusivity in normal-appearing white matter investigated with diffusion tensor MR imaging in

tuberous sclerosis complex. *AJNR Am J Neuroradiol*. 2007;28(9):1662-1667. [CrossRef]
21. Zikou AK, Xydis VG, Astrakas LG, et al. Diffusion tensor imaging in children with tuberous sclerosis complex: tract-based spatial statistics assessment of brain microstructural changes. *Pediatr Radiol*. 2016;46(8):1158-1164. [CrossRef]
22. Peters JM, Taquet M, Prohl AK, et al. Diffusion tensor imaging and related techniques in tuberous sclerosis complex: review and future directions. *Future Neurol*. 2013;8(5):583-597. [CrossRef]
23. Coban G, Gumeler E, Parlak S, et al. Synthetic MRI in children with tuberous sclerosis complex. *Insights Imaging*. 2022;13(1):115. [CrossRef]